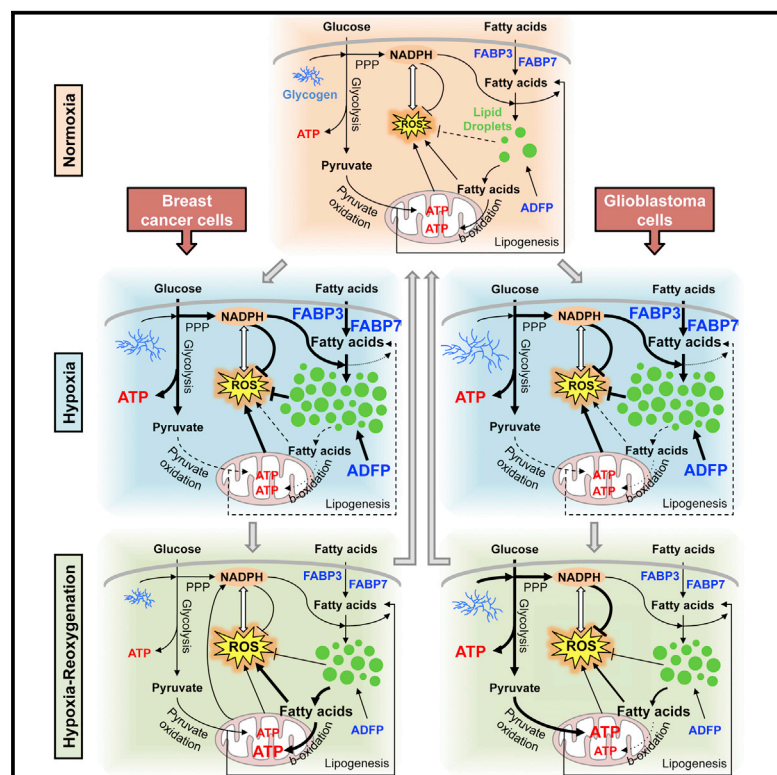


Fatty Acid Uptake and Lipid Storage Induced by HIF-1 α Contribute to Cell Growth and Survival after Hypoxia-Reoxygenation

Graphical Abstract



Authors

Karim Bensaad, Elena Favaro, ..., Almut Schulze, Adrian L. Harris

Correspondence

karim.bensaad@imm.ox.ac.uk

In Brief

Bensaad et al. now show that FABP3 and FABP7 are induced by HIF-1 α and lead to a significant lipid droplet (LD) accumulation in hypoxia. In hypoxia-reoxygenation, ATP production occurs via fatty acid β -oxidation or glycogen degradation in a cell-type-dependent manner, while inhibition of LD formation increases ROS toxicity and decreases cell survival in vitro and strongly impairs tumorigenesis in vivo.

Highlights

FABP3, FABP7, or ADRP induction by HIF-1 α is essential for lipid storage in hypoxia

Lipid storage in hypoxia is due to fatty acid uptake, but not de novo lipid synthesis

Lipid droplets protect against ROS and support survival in hypoxia-reoxygenation

Inhibition of lipid accumulation impairs tumor growth in vivo



Fatty Acid Uptake and Lipid Storage Induced by HIF-1 α Contribute to Cell Growth and Survival after Hypoxia-Reoxygenation

Karim Bensaad,^{1,*} Elena Favaro,¹ Caroline A. Lewis,^{2,7} Barrie Peck,^{2,8} Simon Lord,¹ Jennifer M. Collins,³ Katherine E. Pinnick,³ Simon Wigfield,¹ Francesca M. Buffa,¹ Ji-Liang Li,¹ Qifeng Zhang,⁵ Michael J.O. Wakelam,⁵ Fredrik Karpe,^{3,4} Almut Schulze,^{2,6} and Adrian L. Harris¹

¹CRUK Hypoxia and Angiogenesis Group, The Weatherall Institute of Molecular Medicine, University of Oxford, John Radcliffe Hospital, Headington, Oxford OX3 9DS, UK

²Gene Expression Analysis Laboratory, Cancer Research UK, London Research Institute, 44 Lincoln's Inn Fields, London WC2A 3LY, UK

³Oxford Centre for Diabetes, Endocrinology & Metabolism, University of Oxford, Churchill Hospital, Oxford OX3 7LJ, UK

⁴NIHR Oxford Biomedical Research Centre, OUH Trust, Churchill Hospital, Oxford OX3 7LF, UK

⁵The Babraham Institute, Babraham Research Campus, Cambridge CB22 3AT, UK

⁶Department of Biochemistry and Molecular Biology, Theodor Boveri Institute, Biocenter, Am Hubland, 97074 Würzburg, Germany

⁷Present address: The Koch Institute for Integrative Cancer Research at Massachusetts Institute of Technology, Cambridge, MA 02139, USA

⁸Present address: Functional Genomics Laboratory, Breakthrough Breast Cancer Research Centre, The Institute of Cancer Research, 237 Fulham Road, London SW3 6JB, UK

*Correspondence: karim.bensaad@imm.ox.ac.uk

<http://dx.doi.org/10.1016/j.celrep.2014.08.056>

This is an open access article under the CC BY-NC-ND license (<http://creativecommons.org/licenses/by-nc-nd/3.0/>).

SUMMARY

An *in vivo* model of antiangiogenic therapy allowed us to identify genes upregulated by bevacizumab treatment, including Fatty Acid Binding Protein 3 (*FABP3*) and *FABP7*, both of which are involved in fatty acid uptake. *In vitro*, both were induced by hypoxia in a hypoxia-inducible factor-1 α (HIF-1 α)-dependent manner. There was a significant lipid droplet (LD) accumulation in hypoxia that was time and O₂ concentration dependent. Knockdown of endogenous expression of *FABP3*, *FABP7*, or Adipophilin (an essential LD structural component) significantly impaired LD formation under hypoxia. We showed that LD accumulation is due to *FABP3/7*-dependent fatty acid uptake while *de novo* fatty acid synthesis is repressed in hypoxia. We also showed that ATP production occurs via β -oxidation or glycogen degradation in a cell-type-dependent manner in hypoxia-reoxygenation. Finally, inhibition of lipid storage reduced protection against reactive oxygen species toxicity, decreased the survival of cells subjected to hypoxia-reoxygenation *in vitro*, and strongly impaired tumorigenesis *in vivo*.

INTRODUCTION

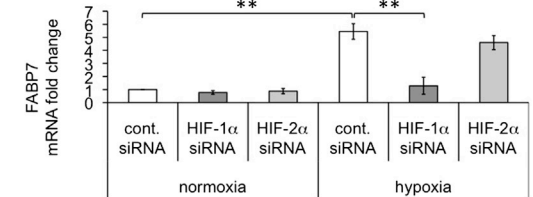
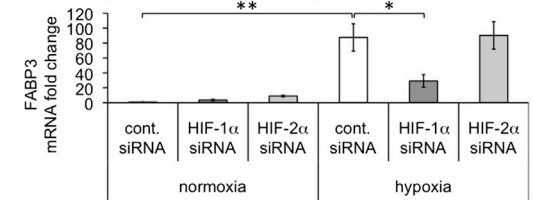
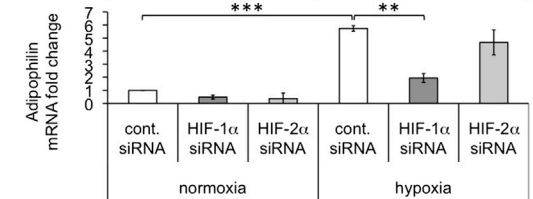
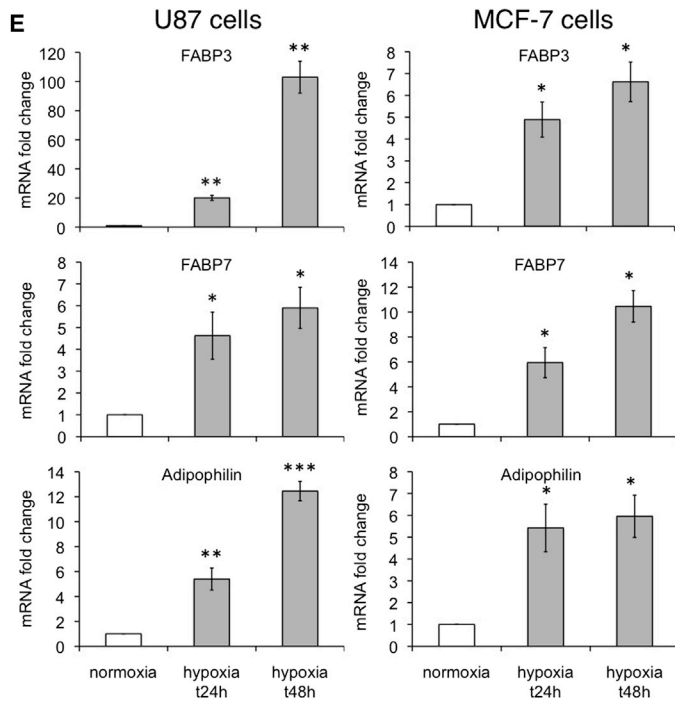
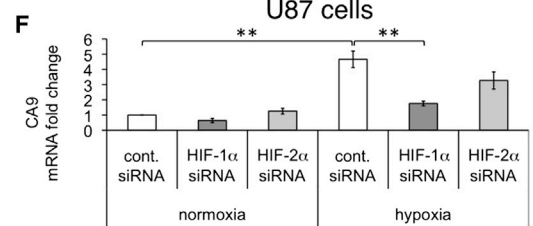
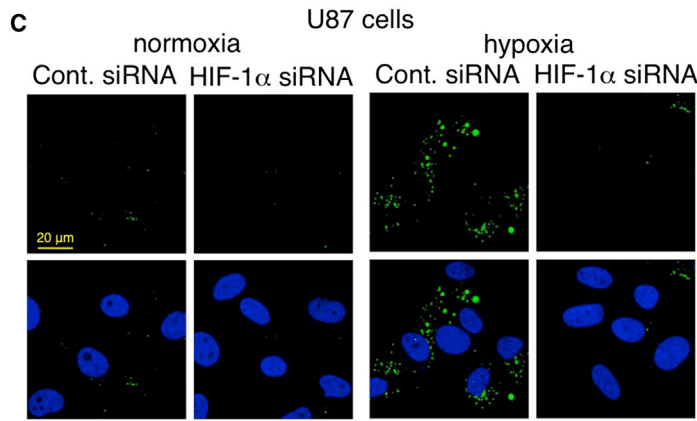
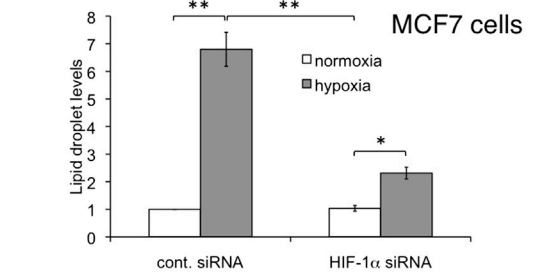
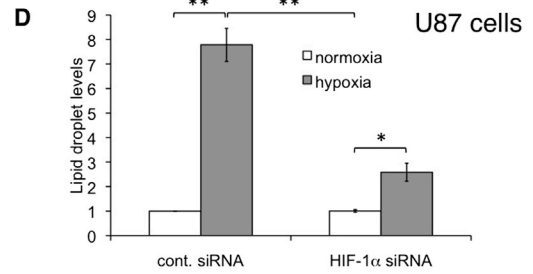
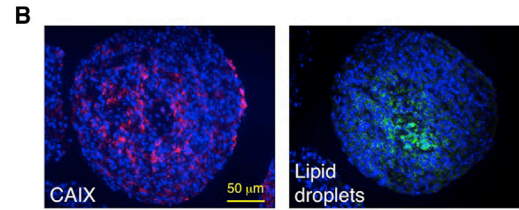
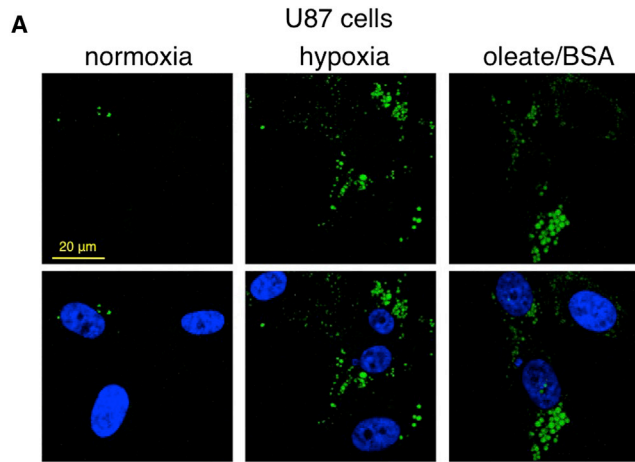
Normal cells produce energy mainly through oxidative phosphorylation (OXPHOS) in the mitochondria. Most cancer cells undergo a metabolic shift toward glycolysis to produce energy, and toward anabolic pathways to synthesize proteins and lipids. Both of these processes promote rapid tumor cell growth (Cairns *et al.*, 2011). The upregulation of glycolysis in normoxic cancer

cells is known as the Warburg effect (Koppenol *et al.*, 2011), a phenomenon that is characterized by an increased glycolytic flux with lactate production from pyruvate even in the presence of abundant O₂ (Vander Heiden *et al.*, 2009).

Oncogenes upregulate the transcription of various glycolytic genes (Levine and Puzio-Kuter, 2010), and the tumor suppressor p53 has a role in regulating glycolysis and OXPHOS (Maddocks and Vousden, 2011; Vousden and Ryan, 2009).

Hypoxia also has a major role in metabolic reprogramming of tumor cells and is considered to be a hallmark of cancer (Hahn and Weinberg, 2011). The hypoxic environment of a tumor leads to stabilization of the hypoxia-inducible factor-1 α (HIF-1 α). HIF-1 α stimulates glycolysis through induction of glucose transporters (GLUT) and glycolytic enzymes (hexokinase-2 [HK2], phosphofructokinase-1 [PFK1], and lactate dehydrogenase A [LDHA]), and inhibition of mitochondrial respiration by pyruvate dehydrogenase kinase 1 (PDK1) (Semenza, 2010). Tumor hypoxia is mainly caused by defective vasculature in fast-growing tumor tissues, leading to diminished O₂ and nutrient supplies. HIF-1 α initiates angiogenesis by induction of vascular endothelial growth factor (VEGF-A) and other angiogenic factors (Chen *et al.*, 2009; Hickey and Simon, 2006; Rey and Semenza, 2010). Antiangiogenic therapies have been demonstrated to induce hypoxia within tumors, resulting in both increased local invasion and distant metastatic spread (Azam *et al.*, 2010). Understanding the biology of hypoxia induced by such therapies is essential for improving them and discovering new targets to overcome therapy resistance (Bridges and Harris, 2011).

In this work, we used a mouse xenograft model of human U87 glioblastoma cells established in severe combined immunodeficiency (SCID) mice, which recapitulates the clinical pattern of initial tumor stabilization on anti-VEGF therapy followed by regrowth and resistance. We used bevacizumab, a monoclonal antibody that recognizes and inhibits all human VEGF isoforms.



(legend on next page)

To analyze the effects of chronic bevacizumab therapy in tumors that had grown through early growth arrest, we identified upregulated genes using an Affymetrix array for human genes. Many genes that are already known to be HIF-1 α targets were induced, including genes involved in metabolic processes (Gordan et al., 2007; Stubbs and Griffiths, 2010). Surprisingly, numerous genes involved in glycogen and lipid metabolism were strongly induced, including PYGL and FABP3 and FABP7.

Our goal in this study was to determine the roles of FABP3 and FABP7 in adaptation to hypoxia. We report that hypoxia induces a HIF-1 α -dependent accumulation of lipid droplets (LDs). LD storage in hypoxia is due to induction of adipophilin (ADRP), which is required for the formation of LD membranes, and to uptake of fatty acids (FAs) through induction of FABP3 and FABP7 rather than de novo FA synthesis. We showed that ATP production occurs via β -oxidation or glycogen degradation in a cell-type-dependent manner in hypoxia-reoxygenation. Finally, we analyzed the effect of inhibiting LD accumulation in hypoxia-reoxygenation, and found that lipid storage is essential for protection against reactive oxygen species (ROS) toxicity, cell survival, and tumor growth.

RESULTS

Analysis of Genes Induced by Hypoxia Resulting from Bevacizumab Therapy in U87 Xenografts

Analysis of genes induced after bevacizumab therapy in U87 xenografts showed an induction of expression of many genes, HIF-1 α upregulation, and induction of necrosis, validating the idea that in vitro pathways can be regulated in vivo in cancer (Li et al., 2011). Gene-expression analysis showed that numerous HIF-1 α targets were induced, including CA9 (Tan et al., 2009). HIF-1 α targets involved in metabolic pathways were among the most upregulated genes (Table S1).

A link between increased lipid metabolism and development of cancer has been reported many times (Swinnen et al., 2006). In cancer cells, several enzymes involved in de novo FA synthesis are either upregulated or activated, and lipogenesis is active (Menendez and Lupu, 2007). However, these enzymes were not induced after bevacizumab treatment. Instead, genes involved in FA desaturation, elongation, uptake, and transport were upregulated. In particular, FABP3 and FABP7, which are essential for FA uptake, showed some of the highest fold changes (Table S1). They are part of a larger family of cytoplasmic proteins comprising nine members (FABP1–FABP9) (Smathers and Petersen, 2011; Storch and McDermott, 2009). FABPs are expressed in a tissue-specific manner, with breast,

muscle, and heart distribution for FABP3, and brain distribution for FABP7 (Smathers and Petersen, 2011; Storch and McDermott, 2009). Strong evidence suggests a broad role for FABPs in the intracellular transport and metabolism of long-chain FA (LCFA). More specifically, the role of FABP3 is evident from the phenotype of FABP3 knockout mice, which show a rate of palmitate uptake reduced by 50% in cardiac myocytes and reduced muscle β -oxidation (Binas et al., 1999). FABP7 binds long-chain polyunsaturated FA (PUFA), allowing uptake and intracellular trafficking (Xu et al., 1996), and is involved in proliferation and invasion of melanoma cells (Slipicevic et al., 2008). High expression of FABP7 in glioblastomas is associated with poor prognosis and more invasive tumors (Kaloshi et al., 2007).

Hypoxia Induces a HIF-1 α -Dependent Accumulation of LDs in Tumor Cells

LDs are dynamic lipid storage organelles that are found in most eukaryotic cells. LDs consist of a monolayer of polar lipids (phospholipids and cholesterol) that surrounds a core of neutral lipids, triglycerides (TGs), and sterol esters. We assessed the abundance of LDs in hypoxia (0.1% O₂) as key components of lipid metabolism using LD540, a lipophilic dye based on the Bodipy fluorophore (Spandl et al., 2009). The oleate/bovine serum albumin (oleate/BSA) complex was used as a positive control. LD accumulation was observed after hypoxia in various cell lines (Figures 1A and S1A).

A 3D spheroid system showed a gradient of O₂ characterized by a large hypoxic central area. U87 spheroids showed LD accumulation in the hypoxic core domain, where CAIX was also induced (Figure 1B). Hypoxic cells contained numerous cytoplasmic droplets with the typical electron microscopic appearance of neutral fat (Figure S1B).

Inhibition of HIF-1 α expression led to a decrease in LD levels after hypoxia, as observed by confocal microscopy and fluorescence-activated cell sorting analysis (Figures 1C, 1D, and S1C). We examined the effect of the peptide dimethylxaloylglycine (DMOG), which activates HIF-1 α , and found that DMOG treatment led to LD accumulation (Figure S1D).

FABP3, FABP7, and ADRP Are Induced under Hypoxic Conditions in a HIF-1 α -Dependent Manner

Having determined that LD accumulation in hypoxia occurs in a HIF-1 α -dependent manner, we investigated the genes involved. *Fabp3*, *Fabp7*, and *Adfp* were upregulated after hypoxia at the RNA and protein levels (Figures 1E and S1E). They were induced in a HIF-1 α -dependent but HIF-2 α -independent manner (Figures 1F, S1F, and S1G). FABP7 was more highly expressed in MCF-7

Figure 1. Hypoxia Induces HIF-1 α -Dependent Accumulation of LDs and Increases FABP3, FABP7, and ADRP Expression in Tumor Cell Lines

(A) LD levels in cells cultured in normoxia or hypoxia for 48 hr. LDs and nuclei were stained with LD540 (green) and DAPI (blue), respectively. The oleate/BSA complex (100 μ M for 16 hr; Sigma) was used as a control.

(B) CAIX expression in U87 spheroid revealed by immunofluorescent staining using a specific antibody (red). LDs were stained with LD540 (green). Nuclei were stained with DAPI (blue).

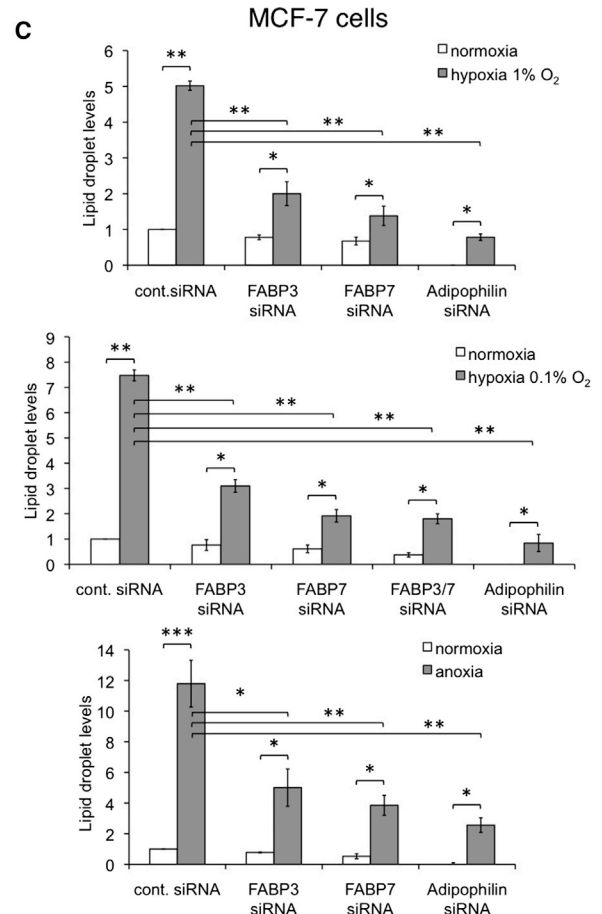
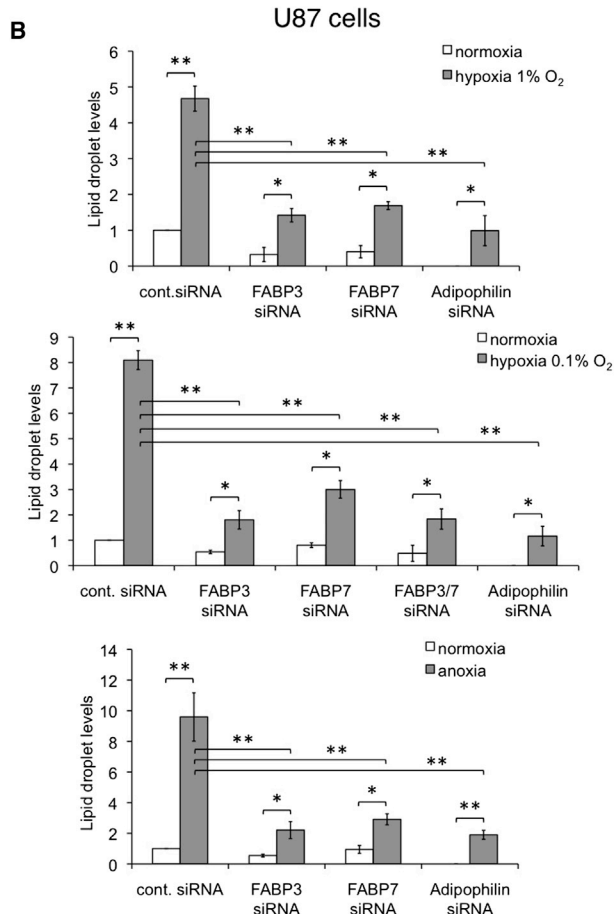
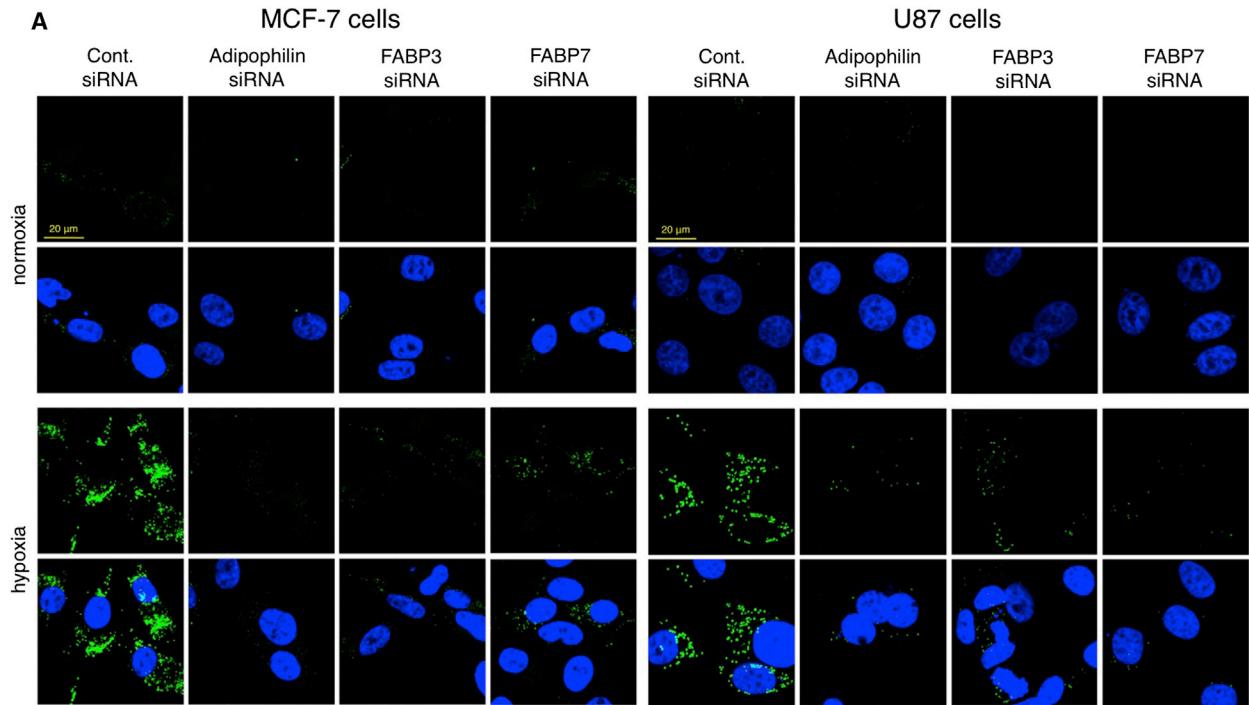
(C) LD levels in cells cultured in normoxia or hypoxia for 48 hr.

(D) LD levels in cells cultured in normoxia or hypoxia for 48 hr.

(E) mRNA levels in cells incubated in normoxia or hypoxia.

(F) mRNA levels in cells incubated in normoxia or hypoxia for 48 hr.

Error bars represent SD. See also Figure S1.



(legend on next page)

cells with undetectable levels of FABP3, whereas FABP3 was more highly expressed in U87 cells with undetectable levels of FABP7. These proteins were also mainly expressed in the spheroid's hypoxic core (Figure S1H).

We previously showed that bevacizumab treatment decreases vessel number in U87 tumor xenografts (Li et al., 2011). Here, we triple stained serial sections of frozen tumor xenografts with DAPI (nucleus), hematoxylin and eosin (H&E), and specific antibodies (Figure S1I). In bevacizumab-treated U87 xenografts, staining for the hypoxia marker pimonidazole revealed clear hypoxic regions surrounding necrotic areas (Figure S1I), whereas untreated tumors showed numerous blood vessels and no pimonidazole staining (data not shown). ADRP, FABP3, and to a lesser extent FABP7 stainings colocalized with pimonidazole in hypoxic regions of U87-treated xenografts (Figure S1I), but not in control xenografts (data not shown).

FABP3, FABP7, and ADRP Are Essential for the Formation of LDs under Hypoxic Conditions

To determine whether FABP3, FABP7, and ADRP are required for LD accumulation in hypoxia, we inhibited their expression using pools of specific small interfering RNA (siRNA) (Figure S2A). Knockdown of FABP3, FABP7, or ADRP expression in U87 and T98G (glioblastoma cell lines), or in MCF-7 and MDA-MB-231 cells (breast cancer cell lines) significantly decreased the formation of LD after hypoxia, as shown by confocal microscopy (Figures 2A and S2B). Flow-cytometric analysis of LD formation showed the same results (Figures 2B, 2C, and S2C). We observed an inverse correlation between O₂ concentration and LD levels with the highest levels observed in anoxic cells (Figures 2B and 2C). In these experiments, we used the ADRP siRNA results in normoxia as the baseline LD standard to normalize the data, as no LD was detectable by microscopy. The effect of FABP3 inhibition on LD storage was more pronounced in U87 cells, and the effect of FABP7 depletion was more marked in MCF-7 cells, a result that paralleled protein and RNA expression (Figures 2B and 2C). We noticed that the combination of FABP3 and FABP7 siRNAs in cotransfection experiments did not enhance the results observed with individual knockdowns (Figures 2B and 2C).

LD Accumulation in Hypoxia Is due to FA Uptake while De Novo Lipid Synthesis Is Repressed

Sterol regulatory element binding protein 1 (SREBP1) and SREBP2 regulate lipid and cholesterol metabolism gene expression by binding to sterol regulatory elements. SREBP activity is subject to a feedback regulation by sterols through regulated intramembrane processing of the inactive precursor (Ben-gochea-Alonso and Ericsson, 2007). When cells are grown in medium supplemented with 1% lipoprotein-deficient serum (LPDS) instead of full serum, SREBPs are activated due to the alleviation of sterol inhibition (Yang et al., 2002).

As expected, normoxic cells cultured in LPDS medium showed a small but significant increase in LD levels, probably via induction of endogenous lipogenesis through SREBP1/2 activation (Figures 3A and S3A). In contrast, LD formation in hypoxia was markedly impaired using LPDS (Figures 3A and S3A), and specific knockdowns did not lead to decreased LD levels in hypoxia in LPDS medium (Figures 3A and S3A). These results show that extracellular FAs are required for LD accumulation in hypoxia. Fatostatin, a small molecule that inhibits the activation of SREBPs (Kamisuki et al., 2009), was used to analyze whether LD changes obtained with LPDS were SREBP1 dependent (Figures 3B and S3B). In normoxia, induction of LD accumulation by LPDS was reduced by Fatostatin, whereas no significant change in LD levels was observed in hypoxia, showing that the LD buildup in hypoxia was SREBP independent (Figures 3B and S3B). The profile of TG species with various acyl carbon and double-bond numbers, and total TG levels showed a significant increase in the rate of hypoxia-stimulated TG synthesis (Figures 3C and S3C). We also noticed differences between cell lines for specific TG species. TGs with three double bonds showed significantly decreased levels in hypoxia in MCF-7 cells, but were significantly increased in U87 cells (Figure 3C). In addition, the metabolic conversion of labeled precursor pyruvate to lipids was significantly decreased in hypoxia (Figure 3D), and the uptake of deuterium from heavy water into TGs was significantly decreased in hypoxia (Figure S3D). Furthermore, hypoxia decreased the activity of the O₂-dependent stearoyl-CoA desaturase-1 (SCD1) (Figure S3E). SCD1 flux, as measured by the ratio C16:1/C16:0 (SCD index), was significantly inhibited by hypoxia (Figure S3E). Altogether, these results indicate that pyruvate-dependent de novo lipogenesis (DNL) is not the origin of the LD accumulation in hypoxia.

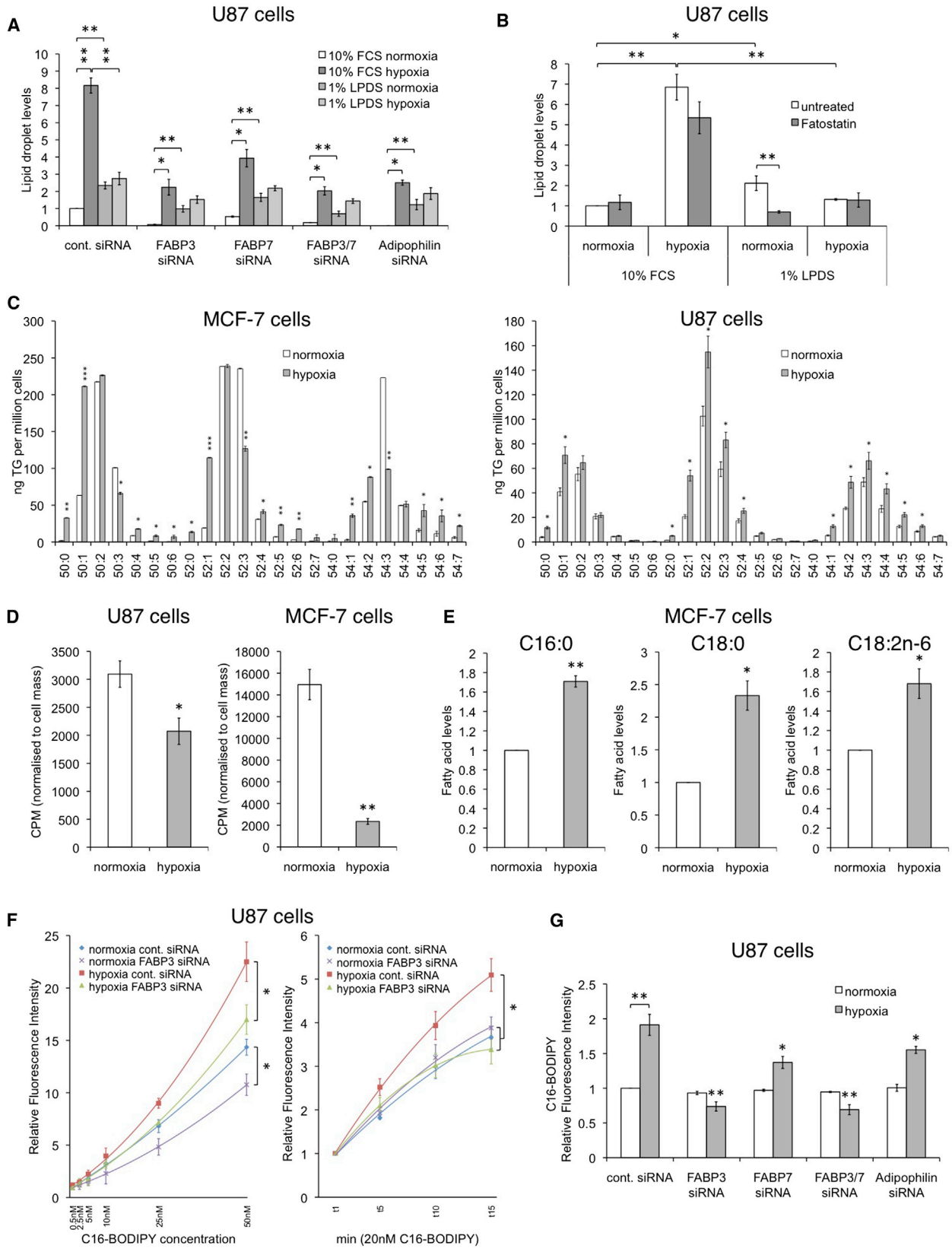
Next, we assessed the effect of the exposure to hypoxia on FA composition in cells by gas chromatography (GC). Levels of palmitate (C16:0), stearate (C18:0), and linoleate (C18:2n-6) were significantly increased in hypoxia (Figure 3E). Palmitate and stearate are saturated FAs. Linoleate, an essential PUFA, cannot be synthesized by mammalian cells and needs to be acquired from the diet. This result is clearly consistent with an increased FA uptake in hypoxia.

FABPs are involved in FA uptake and transport, and ADRP can also stimulate LCFA uptake (Gao and Serrero, 1999). Therefore, we measured FA uptake in hypoxia using a fluorescent palmitate analog (C16-BODIPY). Its uptake was clearly increased in a dose- and time-dependent fashion under all transfection and O₂ tension conditions. C16-BODIPY uptake was significantly enhanced in hypoxia (Figure 3F). FABP3, FABP7, and ADRP knockdowns resulted in decreased C16-BODIPY uptake (Figures 3F, 3G, and S3F).

Recently, a switch from pyruvate oxidation to reductive glutamine metabolism for DNL was shown in hypoxia (Metallo et al., 2012). Therefore, we examined LD formation with or without

Figure 2. FABP3, FABP7, and ADRP Are Essential for the Formation of LDs under Hypoxic Conditions

(A) LD levels in cells cultured in normoxia or hypoxia for 48 hr. LDs were stained with LD540 (green). Nuclei were stained with DAPI (blue).
(B) LD levels in U87 cells cultured in normoxia, hypoxia (0.1 or 1% O₂), or anoxia for 48 hr.
(C) LD levels in MCF-7 cells cultured in normoxia, hypoxia (0.1 or 1% O₂), or anoxia for 48 hr.
Error bars represent SD. See also Figure S2.



(legend on next page)

glutamine in medium, and observed no statistically significant difference between culture conditions (Figure S4G), and no role for glutamine in hypoxic LD formation.

These results suggest that induction of FABP3 or FABP7 is required for FA uptake and LD accumulation in hypoxia. These data, in conjunction with the limited role of SREBPs in hypoxia, demonstrate that LD accumulation is due to extracellular FA uptake rather than de novo synthesis.

FABP3, FABP7, and ADRP Are Essential for Cell Growth in Conditions of Hypoxia and Hypoxia-Reoxygenation

The observation that FABPs induce FA uptake in hypoxia suggests that the resulting LD accumulation is an adaptive response to hypoxic conditions and could play an important role in cell survival.

We measured LD levels in a panel of eight different breast cancer cell lines based on cancer subtype and estimated the cell numbers in normoxia and hypoxia (Figure S4A). The breast cancer cell lines showed higher LD levels than a noncancerous breast cancer cell line (MCF10a), and triple-negative cell lines showed higher basal levels of LD than receptor-positive cell lines. Finally, higher LD levels correlated with an increased ability of breast cancer cells to survive under hypoxia (Figure S4A).

We did not observe a great effect on cell number after our target proteins were silenced in cells continuously cultured in normoxia or hypoxia (Figures 4A and S4B). Interestingly, greater effects were revealed in spheroid and clonogenic assays. We assessed the effect of ADRP, FABP3, and/or FABP7 knockdown on 3D growth by using a spheroid model that closely mimics the tumor microenvironment and hypoxic range (Figures 4B and S4C). Inhibition of LD accumulation using specific siRNAs led to a significant decrease in spheroid size (Figures 4B and S4C). The clonogenic assay showed that the knockdowns significantly reduced the number of cells that were able to form colonies (Figure 4C). Intriguingly, this inhibition was more significant in cells incubated in hypoxia. In the clonogenic assay experiment, cells were grown for 3 days in hypoxia and then for 10 days in normoxia (Figure 4C). This hypoxia-reoxygenation step explained the stronger effect on cell survival observed in the clonogenic assay compared with the proliferation assay.

Taken together, these data demonstrate that prevention of LD formation had a greater effect on cell growth during reoxygenation (Figure 4C) than hypoxia alone (Figure 4A). Hypoxia-reoxygenation phases characterize the intermittent hypoxia that tumors undergo due to an abnormal vascularization resulting in the disruption of blood flow. After inhibiting the expression of FABP3, FABP7, or ADRP, we placed the cells in hypoxia and assessed the cell number after reoxygenation over time. Control

cells showed the highest increase in cell number after 2 days of reoxygenation, and a slower recovery rate was observed for cells with low hypoxic LD levels caused by specific knockdowns (Figures 4D and S5A). We also assessed cell viability using the trypan blue exclusion test. There were delays in growth after hypoxia and recovery after reoxygenation in both cell lines. A decrease in cell viability after specific knockdown associated with a decrease in cell number, which was maintained during the recovery phase, was observed only in MCF7 cells (Figure S4D).

Taken together, these results suggest that lipid storage in hypoxia is essential for cell recovery after restoration of normoxic levels of O₂ to hypoxic cells.

FAs and Glycogen Stored during Hypoxia Are Essential for ATP Production and Survival in Hypoxia-Reoxygenation

We determined the rate of disappearance of LDs during hypoxia-reoxygenation. As expected, depletion of FABP3, FABP7, or ADRP significantly decreased the formation of LDs after 2 days of hypoxia (Figure 5A). During reoxygenation, LD levels gradually returned to those observed in normoxic conditions after 4 days in culture (Figure 5A).

The lipolysis of TGs to free FAs enables the production of ATP in the mitochondria via β -oxidation. Therefore, it seems likely that the regulation of LD levels may play a key role in regulating ATP levels. In control cells, we noted a strong increase in ATP levels after hypoxia-reoxygenation, reaching normoxic values after only 24 hr (Figures 5B and S5A). In breast cancer cells, the reduction of LD levels was inversely proportional to an increase in ATP levels during reoxygenation, and MCF-7 and MDA-MB-231 cells deficient for hypoxic LD accumulation showed a moderate increase in ATP production (Figures 5B and S5A). No such significant difference was noticed in U87 or T98G cells (Figures 5B and S5A). Cells were treated with etomoxir (EX) (Figures 5C, 5D, S5A, and S5B) or trimetazidine (TMZ) (Figures 5C, 5D, and S5C), two specific inhibitors of FA β -oxidation. In breast cancer cells, the results showed the same extent of growth inhibition and reduced ATP levels after reoxygenation as observed after specific knockdowns, whereas no such effect was observed in glioblastoma cells (Figures 5C, 5D, and S5A–S5C). Similarly, there was no effect on viable cell number in U87 cells compared with MCF-7 cells (data not shown).

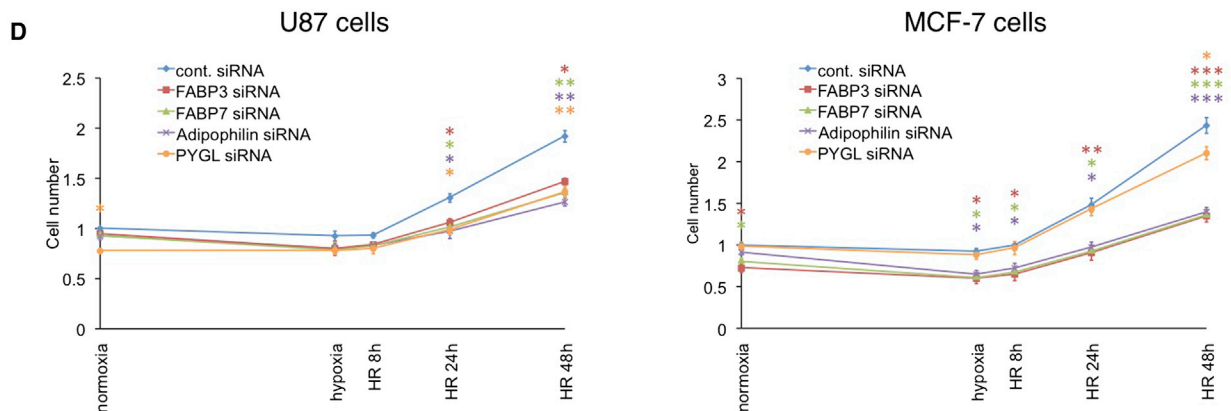
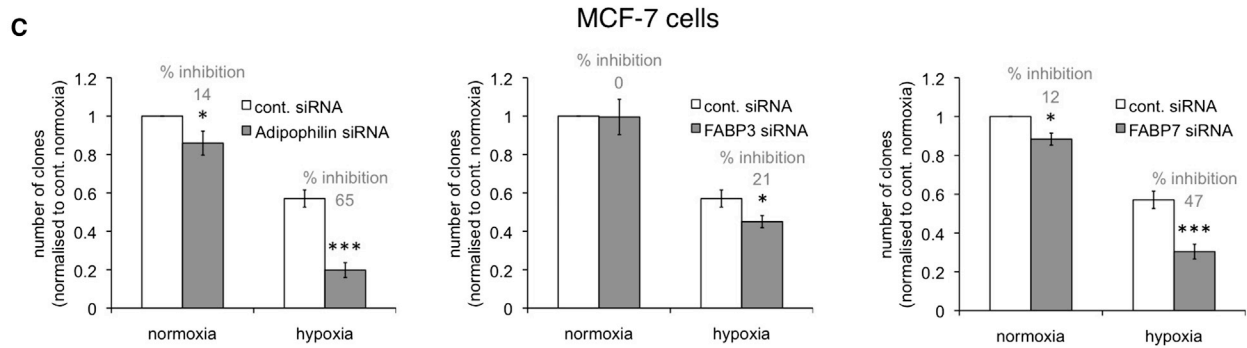
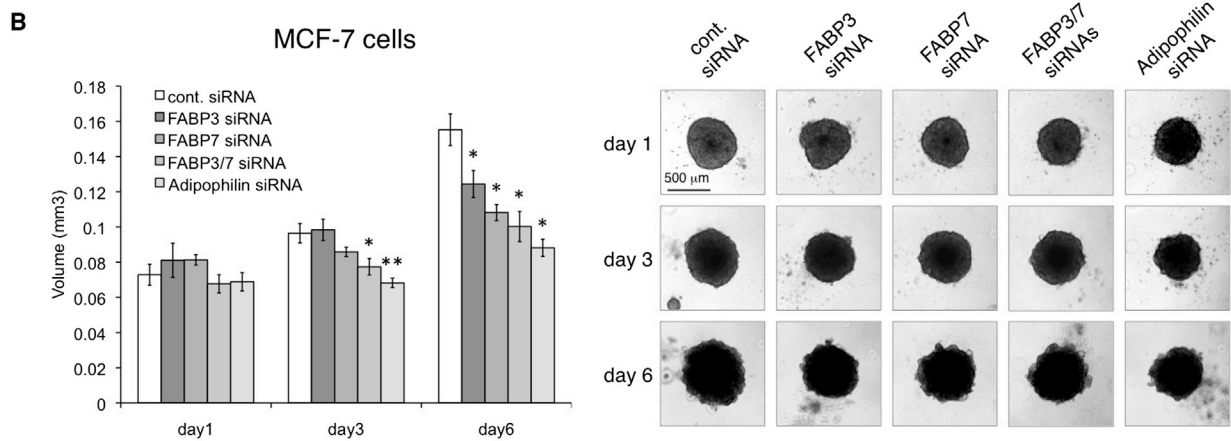
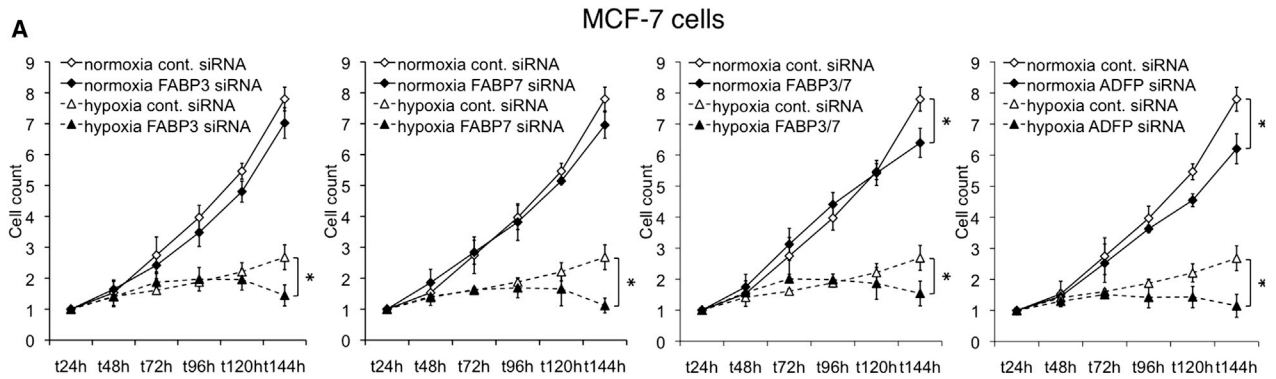
This result suggests that the poor recovery of LD-deficient breast cancer cells after hypoxia-reoxygenation is at least partly due to lack of ATP production via β -oxidation.

To further investigate the discrepancy between cell types regarding ATP production, we directly measured β -oxidation

Figure 3. LD Accumulation under Hypoxic Conditions Is due to FA Uptake, but Not DNL

- (A) LD levels in cells cultured in normoxia or hypoxia, 10% FCS, or 1% LPDS medium for 48 hr.
 (B) LD levels in cells cultured in normoxia or hypoxia, 10% FCS, or 1% LPDS medium, and treated with or without Fatostatin (20 μ M, catalog no. 341329; Calbiochem) for 48 hr.
 (C) TG levels in cells cultured in normoxia or hypoxia for 48 hr.
 (D) Incorporation of [2-¹⁴C]-pyruvate into cellular lipids was measured in counts per minute for cells cultured in normoxia or hypoxia for 24 hr (CPM).
 (E) Palmitate (C16:0), stearate (C18:0), and linoleate (C18:2n-6) levels in cells cultured in normoxia or hypoxia for 48 hr.
 (F) C16-BODIPY uptake in cells cultured in normoxia or hypoxia for 48 hr after FABP3 knockdown.
 (G) C16-BODIPY uptake in cells cultured in normoxia or hypoxia for 48 hr.

Error bars represent SD. See also Figure S3.



(legend on next page)

flux after 2 days of normoxia/hypoxia, with or without reoxygenation, using EX has a control (Figure 5E). In normoxia, FA oxidative flux was 30-fold greater in MCF-7 compared with U87 cells, whereas hypoxia induced a decreased flux in both cell lines (Figure 5E). Importantly, hypoxia-reoxygenation led to an increased β -oxidation flux in MCF-7 compared with hypoxia (Figure 5E).

We previously showed that glycogen metabolism is upregulated in response to hypoxia through the induction of Glycogen Synthase 1 (GYS1) and PYGL, and that metabolism of glucose via glycogen sustains the pentose phosphate pathway, leading to ROS removal and cell proliferation (Favaro et al., 2012). The increased glycogen stores in hypoxia could provide an alternative energy source during hypoxia-reoxygenation. Glycogen levels were higher in U87 compared with MCF-7 cells (Figures 5F and S1B), and increased levels in hypoxia were followed by a regular decrease over time in reoxygenated cells, reaching normoxic levels after 3 days (Figure 5F). We transfected cells with PYGL siRNA to inhibit glycogen degradation and usage, leading to glycogen accumulation in all O₂ concentrations (Figure 5F). Inhibition of PYGL expression decreased both cell number and ATP levels after hypoxia-reoxygenation in U87 cells, but not in MCF-7 cells (Figures 4D and 5B).

In normoxia, treatment with increasing doses of EX led to a strong LD accumulation in MCF-7 cells at higher doses, but only a moderate increase in U87 cells, suggesting a higher flux through β -oxidation in MCF-7 cells (Figure 5G). In hypoxia-reoxygenation, treatment with EX led to slightly higher LD levels compared with untreated U87 cells, whereas a robust LD accumulation was observed in MCF-7 cells (Figure 5H). Furthermore, the knockdown of PYGL led to a quicker rate of disappearance of LDs after hypoxia followed by reoxygenation (Figure 5H).

To further investigate metabolic differences between glioblastoma and breast cancer cells, we used two metabolic inhibitors: 2-deoxyglucose (2-DG), which blocks glycolysis and inhibits pyruvate oxidation due to depletion of pyruvate, and oligomycin, an ATP synthase inhibitor that abolishes OXPHOS and β -oxidation. 2-DG induced a severe decrease in ATP levels in U87 cells in hypoxia-reoxygenation, even at low doses, whereas the inhibitory effect on cell number was similar in both cell lines (Figure S5D). Blocking mitochondrial ATP production by oligomycin significantly decreased ATP levels in both cell types during reoxygenation, whereas cell number was only affected for MCF-7 cells (Figure S5E). These results suggest that breast cancer cells are dependent on mitochondrial ATP production via β -oxidation, and glioblastoma cells are dependent on glycolysis and/or OXPHOS for recovery after hypoxia-reoxygenation.

Altogether, these data reveal that cells recovering after hypoxic phases synthesize ATP through different pathways depending on their tissue of origin. In normoxia, ATP generation via glycolysis and OXPHOS seems to be an important mechanism in both cell lines. However, in MCF-7 cells, LDs provide substrates for

energy production via β -oxidation after hypoxia-reoxygenation, whereas U87 cells degrade glycogen to synthesize ATP through glycolysis and/or OXPHOS.

FABP3, FABP7, and ADRP Are Essential for ROS Removal, NADPH Production, and Survival in Conditions of Hypoxia and Hypoxia-Reoxygenation

Nicotinamide adenine dinucleotide phosphate (NADPH) is derived mainly from glucose flux through the pentose phosphate pathway and glutamine flux through the malic enzyme. NADPH is required to generate reduced glutathione (GSH), which is used for antioxidant mechanisms and leads to decreased ROS levels. Several steps in the metabolism of lipids involve oxidation of the reduced form of NADPH. FA synthesis requires NADPH to supply reducing equivalents. Moreover, inhibition of β -oxidation causes depletion of NADPH levels (Smeland et al., 1992; Pike et al., 2011).

We observed increased ROS levels in control hypoxia, with a further increase after short-term hypoxia-reoxygenation and a gradual decrease to normoxic values after 8 hr of reoxygenation (Figures 6A and S6A). Control cells treated with the antioxidants N-acetyl-cysteine (NAC) or the cell-permeable superoxide dismutase (SOD) mimetic MnTMPyP (Figures 6A and S6A) showed a significant decrease in ROS levels. Inhibition of LD formation drastically enhanced ROS levels compared with control (Figures 6A and S6A).

A significant decrease in NADPH levels and a corresponding increased NADP⁺/NADPH ratio were evident in hypoxia (Figures 6B and S6B). FABP3-, FABP7-, or ADRP-depleted cells exhibited a significant decrease in NADPH levels and an increase in the NADP⁺/NADPH ratio (Figures 6B and S6B). These values consistently returned to values comparable to normoxic levels after 4 days of hypoxia-reoxygenation (Figures 6B and S6B).

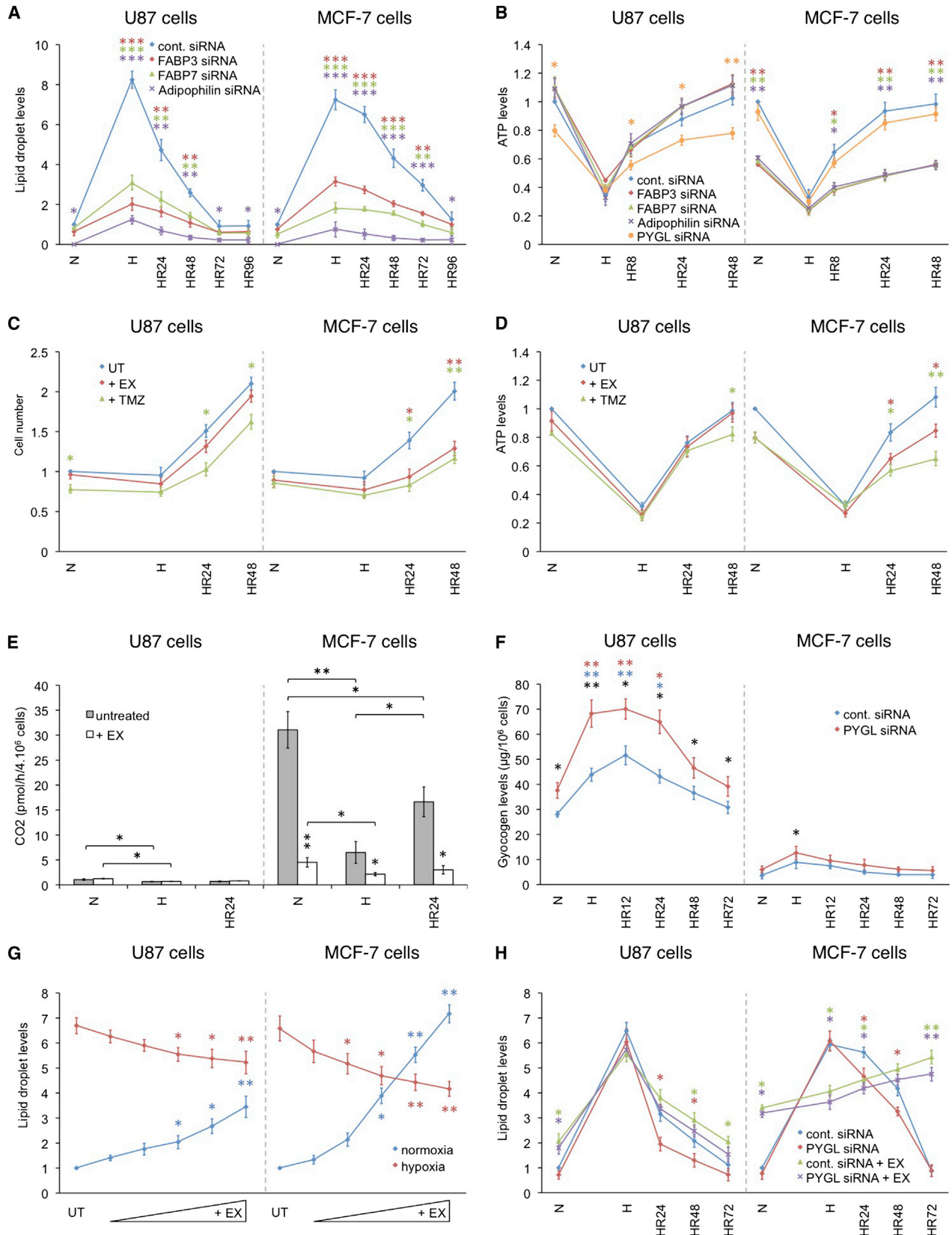
We treated cells with hydrogen peroxide (H₂O₂) in normoxia and observed ROS levels similar to those detected in cells incubated in hypoxia (Figure 6C). When hypoxic cells were incubated in 1% LPDS medium to prevent LD formation, ROS levels were severely induced compared with normoxic or hypoxic cells cultured in normal medium (Figure 6C). For treatment of cells with oleate, we either incubated cells without oleate/BSA for 2 days in hypoxia or preloaded cells with oleate/BSA overnight, before incubation in hypoxia or treatment with H₂O₂. In all situations, the addition of extracellular free FA led to decreased ROS levels (Figure 6C).

To assess whether ROS accumulation also affected cell number as a result of LD depletion, we treated cells with FABP3, FABP7, or ADRP siRNAs with or without antioxidant (Figure 6D). After hypoxia-reoxygenation, treatment led to an increased number of cells depleted for LD (Figure 6D).

Taken together, these results strongly suggest that lack of FA uptake and inhibition of LD storage in hypoxia lead to increased

Figure 4. FABP3, FABP7, and ADRP Are Essential for Cell Survival under Hypoxic Conditions

- (A) Cell counts after 1–6 days in normoxia or hypoxia.
 (B) Volume measurements and microscopy images of spheroids grown for 1–6 days.
 (C) Clonogenic assay for cells cultured in normoxia or hypoxia for 72 hr and then incubated for 10 days in normoxia.
 (D) Cell numbers after 48 hr in normoxia or hypoxia and then incubation in normoxia for 0–48 hr.
 Error bars represent SD. See also Figure S4.



(legend on next page)

levels of ROS. Thus, we conclude that lipid storage is essential for protection against ROS toxicity during hypoxia with or without reoxygenation.

FABP3 or FABP7 Knockdown Impairs the In Vivo Growth of Tumor Xenografts

To determine the in vivo effect of LD depletion, we established U87 cell lines with a stable knockdown of FABP3 or FABP7, and a control, using lentiviral transduction particles containing FABP3 or FABP7 small hairpin RNA (shRNA) expression cassettes and a nontargeting shRNA sequence (Figure S7A). Stable knockdowns significantly decreased the formation of LDs during hypoxia (Figure S7B), cell number after hypoxia-reoxygenation (Figure S7C), and spheroid size (Figure S7D).

We injected the stable cell lines subcutaneously into nude mice and monitored tumor growth. Inhibition of FABP3 or FABP7 expression resulted in a profound delay in tumor growth as compared with the control group (Figures 7A and S7E). In particular, we noticed that tumors in the FABP3/7 shRNA groups reached volumes of 595.1 ± 92.9 and 545.9 ± 94.1 mm³, respectively, after 53 days, whereas volumes in the control group were 610.2 ± 63.3 mm³ after only 35 days (Figure 7A). Tumors in each group were collected when a size of ~ 600 mm³ was reached and examined for expression of various markers.

Tumors derived from U87 cells with stable FABP3 or FABP7 knockdown still showed a decrease in FABP3 or FABP7 mRNA levels (Figure 7B). Furthermore, the expression of FABP3/7 at the RNA level nicely correlated with the size of FABP3/7 shRNA tumors, and some tumors started to grow more rapidly as FABP3/7 expression was restored, whereas shRNA knockdown started to be less efficient after more than 50 days of growth (Figures S7E and S7F).

FABP3 and FABP7 knockdowns led to a significant decrease in levels of necrosis ($7.6\% \pm 3.3\%$ and $22.0\% \pm 4.6\%$, respectively, versus $37.1\% \pm 5.3\%$ for the control group) and hypoxia as determined by pimonidazole staining ($4.4\% \pm 1.1\%$ and $7.8\% \pm 1.9\%$, respectively, versus $20.0\% \pm 5.5\%$ for the control group; Figure 7C). Tumor growth inhibition was also associated with an inhibition in LD formation, as tumors with FABP3 and FABP7 knockdowns showed decreased lipid staining ($1.3\% \pm 0.6\%$ and $1.7\% \pm 0.4\%$, respectively versus $22.3\% \pm 2.2\%$ for the control group; Figure 7C). FABP3 and FABP7 depletions were respectively associated with a significant 1.3-fold and 1.6-fold decrease in the expression of the proliferation-associated marker Ki67 when compared with the control group ($37.2\% \pm 3.0\%$ and $29.7\% \pm 3.4\%$, respectively, versus $48.5\% \pm 2.1\%$ for the control group; Figure 7C). No significant difference among the three groups was observed for expression of

the cell-death-associated marker cleaved caspase-3, excluding the possibility that apoptosis was contributing to tumor growth suppression in vivo (Figure 7C). Altogether, these results suggest that FABP3 and FABP7 represent strong candidates for anti-cancer therapy.

DISCUSSION

In this paper, we report a new role for genes that are induced by hypoxia and involved in FA uptake and lipid storage. We show that LD storage in hypoxia is essential for cell growth and survival in the reoxygenation phase.

FAs can be obtained from the diet or synthesized de novo (Swinnen et al., 2006). In adult, normal, nonadipose tissues, the majority of FAs are acquired from the circulation, and DNL and expression of lipogenic enzymes are low. In contrast, cancer cells exhibit a shift in lipid metabolism as most of the lipogenic enzymes are upregulated or activated. However, we found that the mRNA levels of lipogenic enzymes were not altered after bevacizumab treatment, and pyruvate-dependent DNL was reduced in hypoxia.

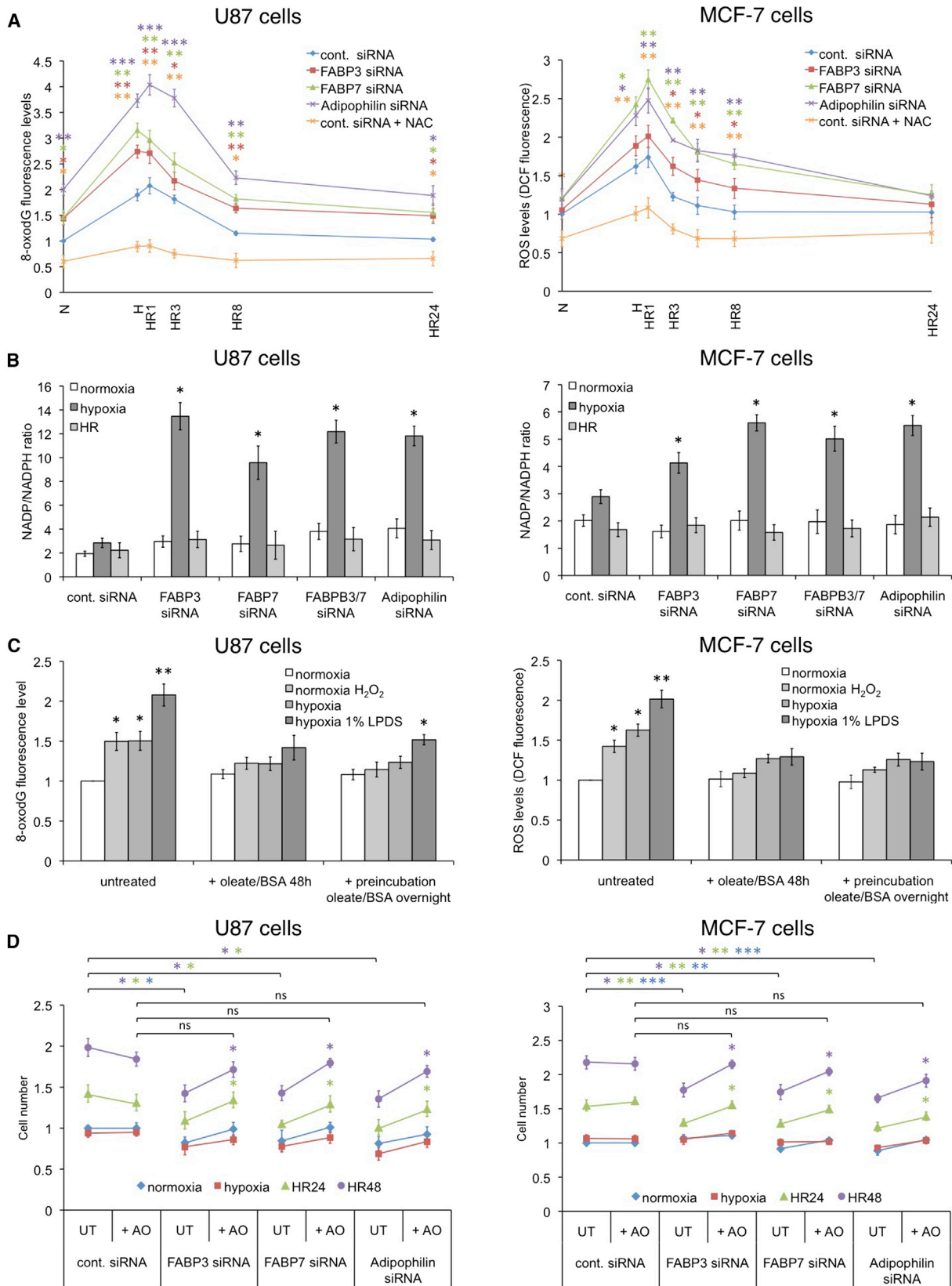
Our results show that hypoxia induces a HIF-1 α -dependent accumulation of LDs in tumor cell lines. LDs have long been recognized, based on light microscopy, to accumulate in hypoxic cells (Zoula et al., 2003), and studies have shown increased lipid metabolism in hypoxia (Laurenti et al., 2011; Mylonis et al., 2012; Shen et al., 2012). TGs contained in LDs are degraded to generate free FAs when cells need to produce ATP via β -oxidation, or to synthesize membranes. Several proteins located at the surface of LDs (HIG2, Perilipin, ADRP, and Tip47) are essential for their membrane integrity (Bozza and Viola, 2010; Farese and Walther, 2009). HIG2 and ADRP are induced by hypoxia (Gimm et al., 2010; Saarikoski et al., 2002). ADRP expression also selectively stimulates LCFA uptake, and its downregulation reduces FA uptake (Faleck et al., 2010; Gao and Serrero, 1999).

FABP3 and FABP7 were upregulated in a murine xenograft antiangiogenic model (Table S1). Several previous works observed that hypoxia was associated with a dependency on extracellular FA and a reduction in de novo FA synthesis (Kamphorst et al., 2013; Young et al., 2013). Nevertheless, we establish a mechanism by which FABPs lead to FA uptake into hypoxic cells.

A recent study (Metallo et al., 2012) showed a switch between pyruvate oxidation to reductive glutamine metabolism for DNL in hypoxia, but it also showed that tumor cells exhibit an overall decreased DNL in hypoxia. This is in accord with our results showing that DNL is significantly impaired in hypoxia in vitro,

Figure 5. FAs and Glycogen Stored during Hypoxia Are Essential for ATP Production and Survival after Hypoxia-Reoxygenation

- (A) LD levels in cells cultured in normoxia or hypoxia for 48 hr and then incubated in normoxia for 1–4 days.
 (B) ATP levels in cells cultured in normoxia or hypoxia for 48 hr and then incubated in normoxia for 0–48 hr.
 (C) Cell number after 48 hr in normoxia or hypoxia and then incubation in normoxia for 0, 24, or 48 hr \pm Etomoxir (EX, 100 μ M).
 (D) ATP levels in cells cultured in normoxia or hypoxia for 48 hr and then incubated in normoxia for 0–48 hr \pm EX (100 μ M).
 (E) β -oxidation in cells cultured in normoxia or hypoxia for 48 hr and then incubated in normoxia for 0–24 \pm EX (100 μ M).
 (F) Glycogen levels in cells cultured in normoxia or hypoxia for 48 hr and then incubated in normoxia for 0–72 hr.
 (G) LD levels in cells cultured in normoxia or hypoxia with an increasing EX concentration (0, 25, 50, 100, 200, and 400 μ M) for 48 hr.
 (H) LD levels in cells cultured in normoxia or hypoxia for 48 hr and then incubated in normoxia for 1–3 days \pm EX (100 μ M).
 Error bars represent SD. See also Figure S5.



(legend on next page)

and that PDK1/3 are induced by bevacizumab treatment in vivo (Table S1). However, we showed that the major source of LD accumulation in hypoxia is glutamine independent.

We conclude that LD storage is essential for survival after hypoxia-reoxygenation based on the observations that (1) free FAs are critical for ATP production via β -oxidation and (2) increased LD levels protect against ROS toxicity. β -oxidation is energetically very efficient (1 molecule of palmitate yields 129 molecules of ATP) but is O_2 dependent and hence is extremely sensitive to blood flow. ATP production via β -oxidation during hypoxia-reoxygenation was observed only in breast cancer cells. In glioblastoma cells, glycogen stored during hypoxia is the major alternative ATP source through glycolysis/OXPHOS after reoxygenation.

Mitochondrial ROS production increases in hypoxia (Guzy et al., 2005; Guzy and Schumacker, 2006). It is also well established that a sudden restoration of O_2 to hypoxic cells can cause substantial ROS accumulation and cell death (Prabhakar et al., 2010). During β -oxidation, acetyl-CoA enters the TCA cycle, where it is broken down to CO_2 . This produces the reducing equivalent NADH, which fuels mitochondrial respiration, or the reducing equivalent NADPH. It has been reported that inhibition of β -oxidation by EX decreases NADPH levels and increases ROS levels (Pike et al., 2011). Also, FAs can be modulators of cellular production of ROS (Schönfeld and Wojtczak, 2008). Indeed, saturated free FAs, especially free palmitate, lead to the production of ROS. In our work, the addition of oleate protected against ROS cytotoxicity, as channeling of saturated FAs toward TGs stored in LDs directed free FAs away from pathways that lead to ROS production (Listenberger et al., 2003). In addition to ATP or ROS modulation, other mechanisms could explain our observations. The inhibition of FABP3/7 or ADRP could also limit the capacity of cells to handle lipolysis products, inducing ceramide production and cell death.

Intermittent hypoxia can positively modulate cancer development, inducing tumor growth, angiogenic processes, chemoresistance, and radioresistance (Toffoli and Michiels, 2008). The functions of glycogen and lipid storage in cell survival in hypoxia-reoxygenation could be key regulators of cancer cells and potential targets for therapy. In recent years, the lipid metabolism pathway has emerged as a potential target for cancer therapy (Abramson, 2011). Several inhibitors of the lipogenic pathway that exhibit antitumor activity have been discovered using pre-clinical models. In particular, chemical inhibition of FA synthase or acetyl-CoA carboxylase has led to decreased growth and survival in various cancer cell types (Flavin et al., 2010; Wang et al., 2010). Other studies have shown the importance of β -oxidation in the development of cancer (Khasawneh et al., 2009; Samudio

et al., 2010). A recent study also demonstrated that monoacylglycerol lipase (MAGL) drives tumorigenesis through the lipolytic release and remodeling of free FAs, and that exogenous sources of FAs can contribute to malignancy in cancers lacking MAGL activity (Nomura et al., 2010). Other findings suggest that cancer cells can use lipoprotein lipase to acquire free FAs from the circulation by lipolysis, to fuel their growth (Kuemmerle et al., 2011). Our results do not exclude the possibility that diacylglycerol acyltransferases (DGATs) also contribute to TG synthesis. Similarly, although we have shown that DNL is reduced by hypoxia, it is still possible that lipid synthesis at the basal level is a key contributor to growth and survival; thus, it will be of interest to study inhibitors of DAGTs.

Using a murine xenograft model, we obtained extremely promising results showing that in vivo tumorigenesis was impaired when FABP3/7 expression was inhibited. This decreased tumor growth rate was associated with a reduction in overall LD levels in tumors. Thus, FA uptake in hypoxic tumor areas seems to represent a promising target for anticancer therapy. Our work provides justification for the screening and development of specific inhibitors of FABP3 and FABP7, which ideally would be able to block the function of both proteins. It will be of interest to investigate the role of FA oxidation or glycogen metabolism inhibitors in the clinic in combination with antiangiogenic therapy that would produce a hypoxic environment. Such an environment would make these pathways more critical, resulting in synthetic lethality. Drugs designed to inhibit glycogen and/or lipid uptake or storage under intermittent O_2 deprivation, in combination with other established agents, may be beneficial for cancer therapy.

EXPERIMENTAL PROCEDURES

Tissue Culture and Hypoxic Conditions

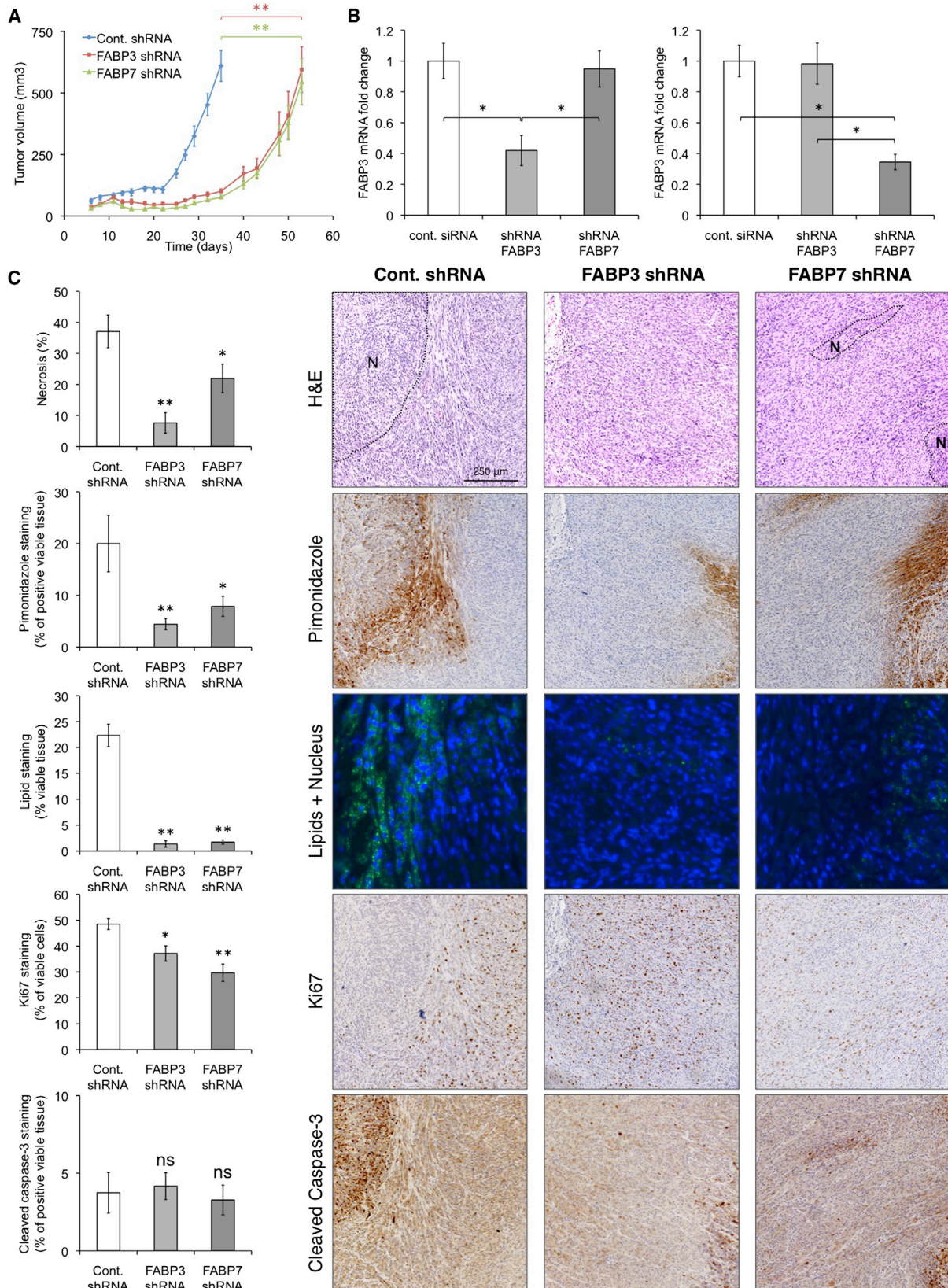
Cells were cultured at 37°C in Dulbecco's modified Eagle's medium (DMEM; GIBCO), 10% fetal calf serum (FCS), 50 U/ml of penicillin, and 50 g/ml of streptomycin. Cell exposure to hypoxia (0.1% O_2) was undertaken in an INVIVO2 400 hypoxic workstation (Ruskin Technology, manufactured for PRO-LAB) using a continuous flow of a humidified mixture of 0.1% O_2 , 5% CO_2 , and 94.9% N_2 .

Staining of LD with LD540

LD540 was developed for microscopic imaging of LD (Spandl et al., 2009). Cells were fixed with 4% paraformaldehyde (PFA) for 15 min, incubated with a solution of 0.05 μ g/ml LD540 (stock solution in ethanol at 0.5 mg/ml) in PBS in the dark at room temperature (RT) for 10 min, and washed three times with PBS. For microscopic analysis, cells were mounted in Vectashield Hard-Set Mounting Medium with DAPI (Vector Laboratories). Images were acquired with a confocal microscope (LSM 510 Confocal Laser Scanning Microscope (Zeiss) or Zeiss Axioskop 2 plus microscope. For flow cytometry, cells were resuspended in PBS and analyzed (CyAn ADP Analyzer; Beckman Coulter).

Figure 6. FABP3, FABP7, and ADRP Are Essential for NADPH Production, ROS Removal, and Survival in Conditions of Hypoxia and Hypoxia-Reoxygenation

- (A) ROS levels in cells cultured in normoxia or hypoxia for 48 hr and then incubated in normoxia for 0–24 hr. NAC, N-acetyl-cysteine (2 mM; Sigma).
 (B) NADP⁺/NADPH ratios in cells cultured in normoxia or hypoxia for 48 hr with or without reoxygenation for 4 days.
 (C) ROS levels in cells were cultured for 48 hr in normoxia, $\pm H_2O_2$ (0.5 mM), or hypoxia, with 10% FCS or 1% LPDS medium. Cells were also left untreated, treated with oleate/BSA (100 μ M) for 48 hr, or preincubated with oleate/BSA (100 μ M) overnight before culture in hypoxia.
 (D) Cell number after 48 hr in normoxia or hypoxia and then incubation in normoxia for 0–48 hr \pm the antioxidant (AO) MnTMPyP (12.5 μ M; Calbiochem).
 Error bars represent SD. See also Figure S6.



(legend on next page)

The mean fluorescence intensity values of the total cell population for each sample were converted to “LD levels” in the graphs.

Clonogenic Assay

Cells were reverse transfected with the indicated siRNAs. At 24 hr after transfection, the medium was changed. Cells were incubated in normoxia or hypoxia for 72 hr and then in normoxia for 10 days. Colonies were counted after staining with 1% crystal violet.

Generation of Spheroids

We used a method to rapidly generate single-tumor spheroids (Ivascu and Kubbies, 2006, 2007). Cells were diluted in ice-cold medium to 2.5×10^4 cells/ml. For MCF-7 cells, Matrigel (BD Biosciences) was thawed on ice and added at a final concentration of 2.5% to the cell suspension. Then, 5,000 cells (200 μ l) of the cell suspension were added to each well of a round-bottom, ultra-low attachment, 96-well plate (Corning). To initiate spheroid formation, the plates were subjected to centrifugation at 1,000 *g* for 10 min. The plates were then incubated at 37°C and 5% CO₂ in a humidified incubator. Images were acquired with a Zeiss Axiovert 135 microscope and volumes were determined with the use of ImageJ software (<http://rsb.info.nih.gov/ij/>).

Cell Viability Assay

To test for cytotoxic effects, we used the trypan blue exclusion test. Cells were incubated in hypoxia for 48 hr and reoxygenated for a further 48 hr. After cell collection, 0.5 ml of cell suspension was added to 50 μ l of 0.4% trypan blue. Viable and dead cells were counted using a Cellometer counting chamber (Nexcelom Bioscience). The percentage of viability was determined by the following equation: % of cell viability = (number of viable cells/total cell number) \times 100.

Lipid Synthesis

Cells were grown in normoxia or 0.1% O₂ for 24 hr. Then, 2.5 μ Ci/ml [2-¹⁴C]-pyruvate (166 μ M final concentration; Perkin Elmer) was added and the cells were incubated for a further 4 hr in the respective O₂ conditions. Cells were washed in 3 \times PBS and lysed in 0.5% Triton X-100. Lipids were extracted by successive addition of 2 ml methanol, 2 ml chloroform, and 1 ml dH₂O. Phase separation was achieved by centrifugation at 1,000 rpm for 15 min. The organic (lower) phase was recovered and dried. Lipids were dissolved in Ultima Gold LSC Cocktail (Perkin Elmer) and counted on a Beckman LS 6500 scintillation counter.

GC Analysis

Cells were incubated for 48 hr under normoxic and 0.1% O₂ conditions. Total lipids were then extracted using the Folch solvent extraction method and TGs were isolated via solid-phase extraction. FA methyl esters (FAMES) of the isolated TG FAs were prepared prior to GC analysis as previously described (Collins et al., 2011). FAs were quantitated by adding 50 μ g internal standard (C15:0 TAG) to each sample prior to extraction and calculating the percentage of recovery proportional to an external standard (50 μ g C23:0 FAME) added to each sample prior to GC analysis.

Lipid Mass Spectrometry

Cellular lipids were extracted using the Folch method. After addition of the appropriate standards, the lipids were separated by normal-phase HPLC and the lipids were identified and semiquantitated by mass spectrometry (MS) using a Thermo Orbitrap mass spectrometer as previously described (Rainero et al., 2012).

DNL Measurement

DNL was calculated based on a method previously described by Lee et al. (1994). Deuterated water (²H₂O) was added to a concentration of 5% to cells for 48 hr. Cells were then harvested and FAMES were prepared prior to GC and GC-MS analysis. The molar enrichment of each TG FA was measured and the percentage of synthesis was calculated based on the observed/theoretical molar enrichment. The amount of DNL-derived FA was then calculated from the total TG FA measured by GC analysis and was expressed as a percentage of the total TG FA.

FA β -Oxidation Measurement

β -oxidation was measured as previously described by Pinnick et al. (2010) using 0.5 mM oleate and 0.5 μ Ci [¹⁴C]oleate (Perkin Elmer) solution bound to BSA in low-glucose DMEM (5 mM). The rate of oxidation was calculated as pmol CO₂/h/4 \times 10⁶ cells.

Uptake of Palmitate

BODIPY FL C16 (Molecular Probes) was diluted at 5 mM in DMSO as a stock solution. After treatment, the culture medium was removed and the cells were washed with PBS and incubated with BODIPY FL C16 in PBS for 15 min at RT. Cells were washed three times with cold PBS and incubated with 4% PFA for 30 min at RT. To determine FA uptake, cells were analyzed by flow cytometry using the FL1-FITC channel (CyAn ADP Analyzer; Beckman Coulter).

Mouse Tumor Study

All protocols were carried out in accordance with Home Office regulations (Li et al., 2011). Female BALB/c SCID mice (Harlan Sprague Dawley, 6–8 weeks old) were injected subcutaneously in the lower flank with 100 μ l of Matrigel (BD Bioscience) and 10⁷ cells suspended in 100 μ l of serum-free medium. Tumor growth was monitored and measured two to three times per week with the use of calipers. Tumor volume was calculated from the formula $V = \text{length} \times \text{width} \times \text{height} \times \pi/6$. When the tumors reached 600 mm³, the mice were sacrificed by cervical dislocation. At 90 min prior to sacrifice, the mice were injected intraperitoneally with 100 mg/kg of pimonidazole (Chemicon International). Immunohistochemistry was carried out as previously described (Li et al., 2011). The following primary antibodies were used: Hypoxyprobe-1 (Chemicon International), Ki67 (Dako), and cleaved caspase-3 (R&D Systems). Slides were incubated with anti-rabbit/anti-mouse secondary antibody (Dako), and DAB (Dako) was applied to the sections for 5–8 min. The slides were counterstained by immersion in a hematoxylin solution (Sigma-Aldrich) and mounted with Aquamount (VWR). Histology slides were scanned with the Hamamatsu NanoZoomer scanner and analyzed quantitatively by image analysis with ImageJ software using color deconvolution (<http://rsb.info.nih.gov/ij/>).

Statistical Analysis

For pooled data, results were expressed as the mean and SD of the mean of at least three independent experiments. Statistics were carried out using Student's *t* test and linear regression of log-transformed growth data (significant difference: **p* < 0.05, ***p* < 0.01, ****p* < 0.001).

SUPPLEMENTAL INFORMATION

Supplemental Information includes Supplemental Experimental Procedures, seven figures, and one table and can be found with this article online at <http://dx.doi.org/10.1016/j.celrep.2014.08.056>.

Figure 7. Inhibition of FABP3 or FABP7 Endogenous Expression Inhibits Cell Proliferation and Impairs Tumor Growth

(A) shRNA U87 cells were injected subcutaneously into BALB/c SCID mice and tumor growth was monitored every 2–3 days. The average size and SEM of seven tumors are represented.

(B) FABP3 and FABP7 mRNA levels in the three mice groups.

(C) From top to bottom: tumor histology (H&E) with necrotic areas indicated by N, tumor hypoxia measured by staining for pimonidazole, LDs stained with LD540 (green) and nuclei stained with DAPI (blue), and tumor cell proliferation and cell death measured by staining for Ki67 and cleaved caspase-3, respectively.

Error bars represent SD. See also Figure S7.

ACKNOWLEDGMENTS

We thank Professor David Ferguson for help with electron microscopy experiments. K.B. was supported by a Cancer Research UK (CRUK) fellowship. E.F. was supported by GlaxoSmithKline. S.L. and J.M.C. were supported by the Breast Cancer Research Foundation and CRUK. Q.Z. and M.J.O.W. were funded by the Biotechnology and Biological Sciences Research Council (BBSRC). This study was supported by CRUK.

Received: December 20, 2013

Revised: July 16, 2014

Accepted: August 22, 2014

Published: September 25, 2014

REFERENCES

- Abramson, H.N. (2011). The lipogenesis pathway as a cancer target. *J. Med. Chem.* *54*, 5615–5638.
- Azam, F., Mehta, S., and Harris, A.L. (2010). Mechanisms of resistance to anti-angiogenesis therapy. *Eur. J. Cancer* *46*, 1323–1332.
- Bengochea-Alonso, M.T., and Ericsson, J. (2007). SREBP in signal transduction: cholesterol metabolism and beyond. *Curr. Opin. Cell Biol.* *19*, 215–222.
- Binas, B., Danneberg, H., McWhir, J., Mullins, L., and Clark, A.J. (1999). Requirement for the heart-type fatty acid binding protein in cardiac fatty acid utilization. *FASEB J.* *13*, 805–812.
- Bozza, P.T., and Viola, J.P. (2010). Lipid droplets in inflammation and cancer. *Prostaglandins Leukot. Essent. Fatty Acids* *82*, 243–250.
- Bridges, E.M., and Harris, A.L. (2011). The angiogenic process as a therapeutic target in cancer. *Biochem. Pharmacol.* *81*, 1183–1191.
- Cairns, R.A., Harris, I.S., and Mak, T.W. (2011). Regulation of cancer cell metabolism. *Nat. Rev. Cancer* *11*, 85–95.
- Chen, L., Endler, A., and Shibasaki, F. (2009). Hypoxia and angiogenesis: regulation of hypoxia-inducible factors via novel binding factors. *Exp. Mol. Med.* *41*, 849–857.
- Collins, J.M., Neville, M.J., Pinnick, K.E., Hodson, L., Ruyter, B., van Dijk, T.H., Reijngoud, D.J., Fielding, M.D., and Frayn, K.N. (2011). De novo lipogenesis in the differentiating human adipocyte can provide all fatty acids necessary for maturation. *J. Lipid Res.* *52*, 1683–1692.
- Faleck, D.M., Ali, K., Roat, R., Graham, M.J., Crooke, R.M., Battisti, R., Garcia, E., Ahima, R.S., and Imai, Y. (2010). Adipose differentiation-related protein regulates lipids and insulin in pancreatic islets. *Am. J. Physiol. Endocrinol. Metab.* *299*, E249–E257.
- Farese, R.V., Jr., and Walther, T.C. (2009). Lipid droplets finally get a little R-E-S-P-E-C-T. *Cell* *139*, 855–860.
- Favaro, E., Bensaad, K., Chong, M.G., Tennant, D.A., Ferguson, D.J., Snell, C., Steers, G., Turley, H., Li, J.L., Günther, U.L., et al. (2012). Glucose utilization via glycogen phosphorylase sustains proliferation and prevents premature senescence in cancer cells. *Cell Metab.* *16*, 751–764.
- Flavin, R., Peluso, S., Nguyen, P.L., and Loda, M. (2010). Fatty acid synthase as a potential therapeutic target in cancer. *Future Oncol.* *6*, 551–562.
- Gao, J., and Serrero, G. (1999). Adipose differentiation related protein (ADRP) expressed in transfected COS-7 cells selectively stimulates long chain fatty acid uptake. *J. Biol. Chem.* *274*, 16825–16830.
- Gimm, T., Wiese, M., Teschemacher, B., Deggerich, A., Schödel, J., Knaup, K.X., Hackenbeck, T., Hellerbrand, C., Amann, K., Wiesener, M.S., et al. (2010). Hypoxia-inducible protein 2 is a novel lipid droplet protein and a specific target gene of hypoxia-inducible factor-1. *FASEB J.* *24*, 4443–4458.
- Gordan, J.D., Thompson, C.B., and Simon, M.C. (2007). HIF and c-Myc: sibling rivals for control of cancer cell metabolism and proliferation. *Cancer Cell* *12*, 108–113.
- Guzy, R.D., and Schumacker, P.T. (2006). Oxygen sensing by mitochondria at complex III: the paradox of increased reactive oxygen species during hypoxia. *Exp. Physiol.* *91*, 807–819.
- Guzy, R.D., Hoyos, B., Robin, E., Chen, H., Liu, L., Mansfield, K.D., Simon, M.C., Hammerling, U., and Schumacker, P.T. (2005). Mitochondrial complex III is required for hypoxia-induced ROS production and cellular oxygen sensing. *Cell Metab.* *1*, 401–408.
- Hanahan, D., and Weinberg, R.A. (2011). Hallmarks of cancer: the next generation. *Cell* *144*, 646–674.
- Hickey, M.M., and Simon, M.C. (2006). Regulation of angiogenesis by hypoxia and hypoxia-inducible factors. *Curr. Top. Dev. Biol.* *76*, 217–257.
- Ivascu, A., and Kubbies, M. (2006). Rapid generation of single-tumor spheroids for high-throughput cell function and toxicity analysis. *J. Biomol. Screen.* *11*, 922–932.
- Ivascu, A., and Kubbies, M. (2007). Diversity of cell-mediated adhesions in breast cancer spheroids. *Int. J. Oncol.* *31*, 1403–1413.
- Kaloshi, G., Mokhtari, K., Carpentier, C., Taillibert, S., Lejeune, J., Marie, Y., Delattre, J.Y., Godbout, R., and Sanson, M. (2007). FABP7 expression in glioblastomas: relation to prognosis, invasion and EGFR status. *J. Neurooncol.* *84*, 245–248.
- Kamisuki, S., Mao, Q., Abu-Elheiga, L., Gu, Z., Kugimiya, A., Kwon, Y., Shinohara, T., Kawazoe, Y., Sato, S., Asakura, K., et al. (2009). A small molecule that blocks fat synthesis by inhibiting the activation of SREBP. *Chem. Biol.* *16*, 882–892.
- Kamphorst, J.J., Cross, J.R., Fan, J., de Stanchina, E., Mathew, R., White, E.P., Thompson, C.B., and Rabinowitz, J.D. (2013). Hypoxic and Ras-transformed cells support growth by scavenging unsaturated fatty acids from lysophospholipids. *Proc. Natl. Acad. Sci. USA* *110*, 8882–8887.
- Khasawneh, J., Schulz, M.D., Walch, A., Rozman, J., Hrabe de Angelis, M., Klingenspor, M., Buck, A., Schwaiger, M., Saur, D., Schmid, R.M., et al. (2009). Inflammation and mitochondrial fatty acid beta-oxidation link obesity to early tumor promotion. *Proc. Natl. Acad. Sci. USA* *106*, 3354–3359.
- Koppenol, W.H., Bounds, P.L., and Dang, C.V. (2011). Otto Warburg's contributions to current concepts of cancer metabolism. *Nat. Rev. Cancer* *11*, 325–337.
- Kuemmerle, N.B., Rysman, E., Lombardo, P.S., Flanagan, A.J., Lipe, B.C., Wells, W.A., Pettus, J.R., Froehlich, H.M., Memoli, V.A., Morganeli, P.M., et al. (2011). Lipoprotein lipase links dietary fat to solid tumor cell proliferation. *Mol. Cancer Ther.* *10*, 427–436.
- Laurenti, G., Benedetti, E., D'Angelo, B., Cristiano, L., Cinque, B., Raysi, S., Alecci, M., Cerù, M.P., Cifone, M.G., Galzio, R., et al. (2011). Hypoxia induces peroxisome proliferator-activated receptor α (PPAR α) and lipid metabolism peroxisomal enzymes in human glioblastoma cells. *J. Cell. Biochem.* *112*, 3891–3901.
- Lee, W.N., Bassilian, S., Guo, Z., Schoeller, D., Edmond, J., Bergner, E.A., and Byerley, L.O. (1994). Measurement of fractional lipid synthesis using deuterated water (2H₂O) and mass isotopomer analysis. *Am. J. Physiol.* *266*, E372–E383.
- Levine, A.J., and Puzio-Kuter, A.M. (2010). The control of the metabolic switch in cancers by oncogenes and tumor suppressor genes. *Science* *330*, 1340–1344.
- Li, J.L., Sainson, R.C., Oon, C.E., Turley, H., Leek, R., Sheldon, H., Bridges, E., Shi, W., Snell, C., Bowden, E.T., et al. (2011). DLL4-Notch signaling mediates tumor resistance to anti-VEGF therapy in vivo. *Cancer Res.* *71*, 6073–6083.
- Listenberger, L.L., Han, X., Lewis, S.E., Cases, S., Farese, R.V., Jr., Ory, D.S., and Schaffer, J.E. (2003). Triglyceride accumulation protects against fatty acid-induced lipotoxicity. *Proc. Natl. Acad. Sci. USA* *100*, 3077–3082.
- Maddocks, O.D., and Vousden, K.H. (2011). Metabolic regulation by p53. *J. Mol. Med.* *89*, 237–245.
- Menendez, J.A., and Lupu, R. (2007). Fatty acid synthase and the lipogenic phenotype in cancer pathogenesis. *Nat. Rev. Cancer* *7*, 763–777.
- Metallo, C.M., Gameiro, P.A., Bell, E.L., Mattaini, K.R., Yang, J., Hiller, K., Jewell, C.M., Johnson, Z.R., Irvine, D.J., Guarente, L., et al. (2012). Reductive glutamine metabolism by IDH1 mediates lipogenesis under hypoxia. *Nature* *481*, 380–384.

- Mylonis, I., Sembongi, H., Befani, C., Liakos, P., Siniouoglou, S., and Simos, G. (2012). Hypoxia causes triglyceride accumulation by HIF-1-mediated stimulation of lipin 1 expression. *J. Cell Sci.* *125*, 3485–3493.
- Nomura, D.K., Long, J.Z., Niessen, S., Hoover, H.S., Ng, S.W., and Cravatt, B.F. (2010). Monoacylglycerol lipase regulates a fatty acid network that promotes cancer pathogenesis. *Cell* *140*, 49–61.
- Pike, L.S., Smift, A.L., Croteau, N.J., Ferrick, D.A., and Wu, M. (2011). Inhibition of fatty acid oxidation by etomoxir impairs NADPH production and increases reactive oxygen species resulting in ATP depletion and cell death in human glioblastoma cells. *Biochim. Biophys. Acta* *1807*, 726–734.
- Pinnick, K., Neville, M., Clark, A., and Fielding, B. (2010). Reversibility of metabolic and morphological changes associated with chronic exposure of pancreatic islet beta-cells to fatty acids. *J. Cell. Biochem.* *109*, 683–692.
- Prabhakar, N.R., Kumar, G.K., and Nanduri, J. (2010). Intermittent hypoxia augments acute hypoxia sensing via HIF-mediated ROS. *Respir. Physiol. Neurobiol.* *174*, 230–234.
- Rainero, E., Caswell, P.T., Muller, P.A.J., Grindlay, J., McCaffrey, M.W., Zhang, Q., Wakelam, M.J.O., Vousden, K.H., Graziani, A., and Norman, J.C. (2012). Diacylglycerol kinase α controls RCP-dependent integrin trafficking to promote invasive migration. *J. Cell Biol.* *196*, 277–295.
- Rey, S., and Semenza, G.L. (2010). Hypoxia-inducible factor-1-dependent mechanisms of vascularization and vascular remodelling. *Cardiovasc. Res.* *86*, 236–242.
- Saarikoski, S.T., Rivera, S.P., and Hankinson, O. (2002). Mitogen-inducible gene 6 (MIG-6), adipophilin and tuftelin are inducible by hypoxia. *FEBS Lett.* *530*, 186–190.
- Samudio, I., Harmancey, R., Fiegl, M., Kantarjian, H., Konopleva, M., Korchin, B., Kaluarachchi, K., Bornmann, W., Duvvuri, S., Taegtmeier, H., and Andreeff, M. (2010). Pharmacologic inhibition of fatty acid oxidation sensitizes human leukemia cells to apoptosis induction. *J. Clin. Invest.* *120*, 142–156.
- Schönfeld, P., and Wojtczak, L. (2008). Fatty acids as modulators of the cellular production of reactive oxygen species. *Free Radic. Biol. Med.* *45*, 231–241.
- Semenza, G.L. (2010). Defining the role of hypoxia-inducible factor 1 in cancer biology and therapeutics. *Oncogene* *29*, 625–634.
- Shen, G.M., Zhao, Y.Z., Chen, M.T., Zhang, F.L., Liu, X.L., Wang, Y., Liu, C.Z., Yu, J., and Zhang, J.W. (2012). Hypoxia-inducible factor-1 (HIF-1) promotes LDL and VLDL uptake through inducing VLDLR under hypoxia. *Biochem. J.* *441*, 675–683.
- Slipicevic, A., Jørgensen, K., Skrede, M., Rosnes, A.K., Trøen, G., Davidson, B., and Flørenes, V.A. (2008). The fatty acid binding protein 7 (FABP7) is involved in proliferation and invasion of melanoma cells. *BMC Cancer* *8*, 276.
- Smathers, R.L., and Petersen, D.R. (2011). The human fatty acid-binding protein family: evolutionary divergences and functions. *Hum. Genomics* *5*, 170–191.
- Smeland, T.E., Nada, M., Cuevas, D., and Schulz, H. (1992). NADPH-dependent beta-oxidation of unsaturated fatty acids with double bonds extending from odd-numbered carbon atoms. *Proc. Natl. Acad. Sci. USA* *89*, 6673–6677.
- Spandl, J., White, D.J., Peychl, J., and Thiele, C. (2009). Live cell multicolor imaging of lipid droplets with a new dye, LD540. *Traffic* *10*, 1579–1584.
- Storch, J., and McDermott, L. (2009). Structural and functional analysis of fatty acid-binding proteins. *J. Lipid Res. Suppl.* *50*, S126–S131.
- Stubbs, M., and Griffiths, J.R. (2010). The altered metabolism of tumors: HIF-1 and its role in the Warburg effect. *Adv. Enzyme Regul.* *50*, 44–55.
- Swinnen, J.V., Brusselmans, K., and Verhoeven, G. (2006). Increased lipogenesis in cancer cells: new players, novel targets. *Curr. Opin. Clin. Nutr. Metab. Care* *9*, 358–365.
- Tan, E.Y., Yan, M., Campo, L., Han, C., Takano, E., Turley, H., Candiloro, I., Pezzella, F., Gatter, K.C., Millar, E.K., et al. (2009). The key hypoxia regulated gene CAIX is upregulated in basal-like breast tumours and is associated with resistance to chemotherapy. *Br. J. Cancer* *100*, 405–411.
- Toffoli, S., and Michiels, C. (2008). Intermittent hypoxia is a key regulator of cancer cell and endothelial cell interplay in tumours. *FEBS J.* *275*, 2991–3002.
- Vander Heiden, M.G., Cantley, L.C., and Thompson, C.B. (2009). Understanding the Warburg effect: the metabolic requirements of cell proliferation. *Science* *324*, 1029–1033.
- Vousden, K.H., and Ryan, K.M. (2009). p53 and metabolism. *Nat. Rev. Cancer* *9*, 691–700.
- Wang, C., Rajput, S., Watabe, K., Liao, D.F., and Cao, D. (2010). Acetyl-CoA carboxylase- α as a novel target for cancer therapy. *Front. Biosci. (Schol. Ed.)* *2*, 515–526.
- Xu, L.Z., Sánchez, R., Sali, A., and Heintz, N. (1996). Ligand specificity of brain lipid-binding protein. *J. Biol. Chem.* *271*, 24711–24719.
- Yang, T., Espenshade, P.J., Wright, M.E., Yabe, D., Gong, Y., Aebersold, R., Goldstein, J.L., and Brown, M.S. (2002). Crucial step in cholesterol homeostasis: sterols promote binding of SCAP to INSIG-1, a membrane protein that facilitates retention of SREBPs in ER. *Cell* *110*, 489–500.
- Young, R.M., Ackerman, D., Quinn, Z.L., Mancuso, A., Gruber, M., Liu, L., Giannoukos, D.N., Bobrovnikova-Marjon, E., Diehl, J.A., Keith, B., and Simon, M.C. (2013). Dysregulated mTORC1 renders cells critically dependent on desaturated lipids for survival under tumor-like stress. *Genes Dev.* *27*, 1115–1131.
- Zoula, S., Rijken, P.F., Peters, J.P., Farion, R., Van der Sanden, B.P., Van der Kogel, A.J., Décorps, M., and Rémy, C. (2003). Pimonidazole binding in C6 rat brain glioma: relation with lipid droplet detection. *Br. J. Cancer* *88*, 1439–1444.